Civil Engineering and Architecture 10(5): 2157-2171, 2022 http://www.hrpub.org
DOI: 10.13189/cea.2022.100534

Numerical Simulation for Flow over A Broad-Crested Weir Using FLOW-3D Program

Nadheer S. Ayoob[1,*], Alaa M. Hamad[2]

[1]Department of Civil Engineering, College of Engineering, Wasit University, Kut, Iraq
[2]Department of Soil and Water Resources, College of Agriculture, Wasit University, Kut, Iraq

Received May 14, 2022; Revised June 14, 2022; Accepted June 24, 2022

Cite This Paper in the Following Citation Styles

(a): *[1] Nadheer S. Ayoob, Alaa M. Hamad , "Numerical Simulation for Flow over A Broad-Crested Weir Using FLOW-3D Program," Civil Engineering and Architecture, Vol. 10, No. 5, pp. 2157-2171, 2022. DOI: 10.13189/cea.2022.100534.*

(b): *Nadheer S. Ayoob, Alaa M. Hamad (2022). Numerical Simulation for Flow over A Broad-Crested Weir Using FLOW-3D Program. Civil Engineering and Architecture, 10(5), 2157-2171. DOI: 10.13189/cea.2022.100534.*

Abstract The free water flow over a broad-crested weir with different down- and upstream inclinations was studied numerically using computational fluid dynamics software (FLOW-3D v11.0.4). Weirs of four various upstream and downstream configurations were investigated to determine the effect of weir shape on the produced coefficient of discharge (C_d), upstream energy grade line (H_1), and depth-averaged flow velocity using five different flow discharges. The obtained numerical results revealed that FLOW-3D program can be depended to simulate the flow over broad-crested weir adequately, as the differences between the numerical and experimental upstream head (h_1) were in the range of 0.0 to 9.6%. Furthermore, reducing upstream slope played an essential role in increasing the discharge coefficient, and reducing the upstream energy grade line (i.e. static pressure above the crest), while downstream inclination showed a negligible influence. Generally, reducing the upstream slope by 50.0 and 70.5% increased discharge coefficient by 9.5 and 13.2%, while decreased the total energy grade line by 4.3 and 8.7%, respectively. According to flow velocity measurement, for the same upstream slope and discharge, the velocity resulted by the weir of inclined upstream and vertical downstream (BRV) was lower than that of the weir of vertical upstream and inclined downstream (VRB) by 28.0%.

Keywords Broad-crested Weir, CFD, FLOW-3D, Flow Velocity, Discharge Coefficient

1. Introduction

Weirs are obstructions built in the way of flowing water. They are simple and common hydraulic devices used mainly for flow control and measurement. Moreover, they can be used for flow diversion, water depth regulation, flood retarding, and energy dissipation.

Weirs can be classified according to their opening shape, emerging nappe. Furthermore, according to their crest shape, weirs are divided into sharp-, narrow-, ogee-, and broad-crested weir (Chow, 1959; Sarker & Rhodes, 2004; Gonzales & Chanson, 2007; Azimi & Rajaratnam, 2009).

A broad-crested weir, as shown in Fig. 1, consists of a flat crest. Broad-crested weir also has a considerable length as compared to thickness of flow passes over its crest (Gonzales & Chanson, 2007). The essential features of a broad-crested weir are:

- Depending on the relative weir length, $\lambda_w = h_1/w$, where w and h_1 are the length of crest and the flow depth with respect to the crest elevation, special flow types can be predicted.
- Approximately stable discharge coefficient (C_d) for $0.1 < \lambda_w < 0.4$.
- Slight sensitivity for the tail water level.
- Inexpensive overshot hydraulic structure (Hager & Schwalt, 1994).

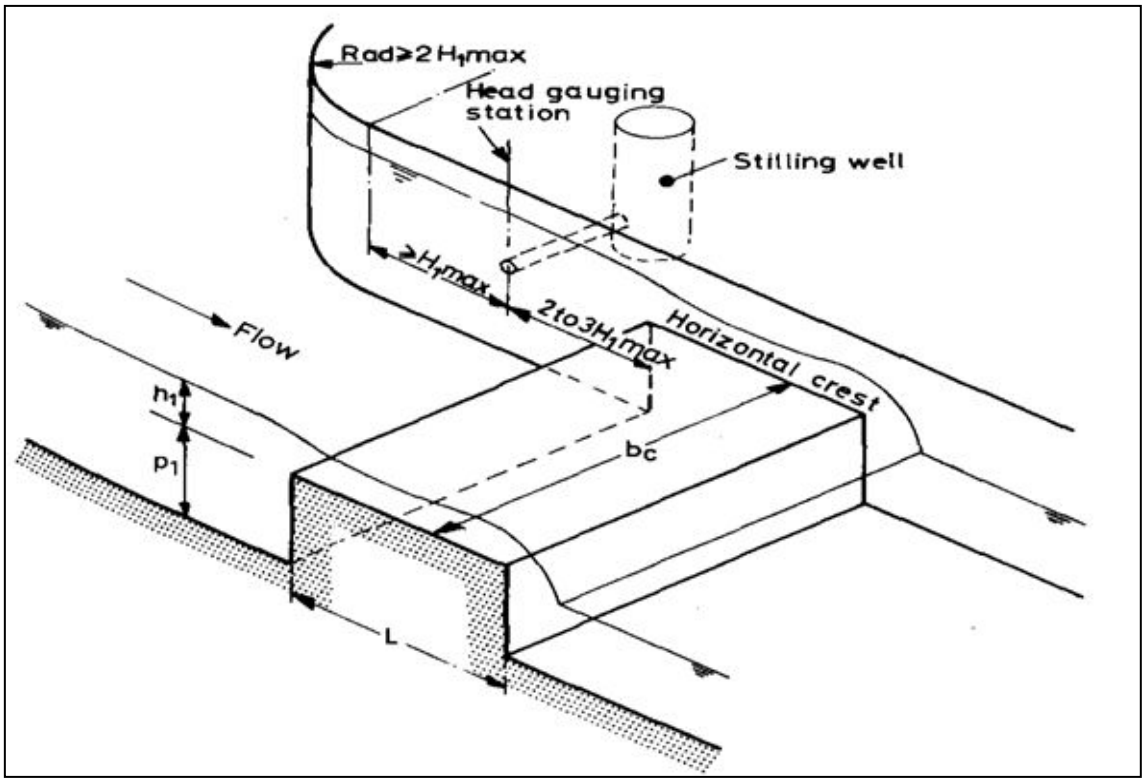

Figure 1. A broad-crested weir (after BSI, 1969).

Many advantages can be obtained by the use of this type of weirs as the following:

- Simple design, construction, and operation hydraulic structure.
- Ability to pass floating debris.
- Suitable measurement device for small to moderate channel work.
- Low head losses as compared to other types of weirs (Huan et al., 2011).

The down- and upstream slopes are considered governing features. They range between a ramp of 1:2 slope (standard embankment type) to a vertical end. Generally, the discharge capacity increases with the increment of upstream face slope (Huan et al., 2011; Ramamurthy et al., 1988; Fritz & Hager, 1998).

Hager et al. (1994) studied experimentally the water flow characteristics over a broad-crested weir. According to this study, the discharge can be determined by the following formula:

$$Q = C_d\, b \sqrt{2g\, H_o^3} \quad (1)$$

where H_o is the total energy above the crest (m), it is calculated using Eq. 2:

$$H_o = h_o + (Q^2/2gb^2[h_o + w]^2) \quad (2)$$

where h_o is upstream water depth above the crest (m), Q is water discharge (m^3/sec), g is acceleration of gravity (m/sec^2), b is width of the weir (m), w is height of the weir (m), C_d is discharge coefficient.

Sargison and Percy (2009) conducted an experimental work to investigate the flow over a broad-crested weir of different down- and upstream slopes using a horizontal laboratory flume. Three various face slopes were studied involved a vertical, 1H:1V, and 2H:1V slopes with different distributions for up- and downstream faces. The obtained results revealed that the slope increment at the upstream face up to the vertical slope significantly lowered the resulted water level so it reduced the static pressure over the weir's crest, and it minimized the discharge coefficient. Nevertheless, the effect of downstream inclination was negligible.

Saker and Rhodes (2004), and Huan et al. (2011) conducted numerical studies to investigate the complicated flow over broad-crested weirs using computational fluid dynamics (CFD) software. Both studies revealed that CFD programs are adequate enough to be depended for analyzing and designing such hydraulic structures.

In fact, there are plenty studies in the provided literature carried out to investigate the flow over broad-crested weirs but the use of CFD programs for this purpose is very rare. Thus, there is an imperative need to evaluate the ability of this program to simulate the complicated flow over broad-crested weirs. The aim of this study is to check the ability of FLOW-3D software to simulate the flow over a broad-crested weir of various up- and downstream inclinations and fixed crest length and width for various flow discharges. Moreover, the study aims to determine discharge coefficient, energy grade line, and flow velocity.

2. Numerical Simulation

2.1. Concept of CFD Application

It is an aspect of fluid mechanics science that uses the computer device to solve the dominant equations of fluid flow (conservation of mass, energy, and momentum) in models of one, two and three dimensions, this is the definition of computational fluid dynamics. Basically, the use of CFD software saves efforts, cost and time because it compensates the preparing of real experiment. Numerical study, typically like experimental study, must simulate the actual conditions for obtaining accurate results.

FLUINT, PHOENICS, FLOW-3D are common examples of CFD programs. In this research, FLOW-3D was depended. It applies numerical methods to solve the equations of fluid motion.

Navier-Stokes equations are approximately the base of FLOW-3D software. These equations solve single-phase fluid flow only. For few earlier decades, different kinds of numerical methods were prepared for simulating the fluid flow depending on finite volume method (FVM), finite element method (FEM), and finite difference method (FDM). FLOW-3D program uses FVM, this method needs small usage of memory, it gives also a faster solution for more complex problem. Numerical model must have a computational mesh or grid. It consists of numerous elements or interconnected cells. The physical zone must be divided by these cells into very small volumes with many nodes. The actual physical space is compensated by numerical one that represented by grid.

Eqs. 3 and 4 show the momentum and continuity equations that depended by FLOW-3D software for solving the required partial differential equations (PDEs):

$$\frac{\partial w}{\partial t} + \frac{1}{V_F}\left\{ u A_x \frac{\partial w}{\partial x} + v A_y R \frac{\partial w}{\partial y} + w A_z \frac{\partial w}{\partial z} \right\} = -\frac{1}{\rho}\frac{\partial P}{\partial z} + G_z + f_z + b_z - \frac{R_{SOR}}{\rho V_F}(w - w_w - \delta w_s) \quad (3)$$

where f_z, f_y, f_x represent the viscous accelerations, G_z, G_y, and G_x represent the body accelerations, and b_z, b_y, and b_x represent the losses of flow across porous baffle plate or through porous media.

$$\frac{V_f}{\rho c^2}\frac{\partial P}{\partial t} + \frac{\partial}{\partial x}(u A_x) + R\frac{\partial}{\partial y}(v A_y) + \frac{\partial}{\partial z}(w A_z) + \xi \frac{u A_x}{x} = \frac{R_{SOR}}{\rho} \quad (4)$$

where R_{SOR} represents the mass source, ρ represents the mass density of fluid, V_f represents the fractional volume open to flow, A_z, A_y, and A_x represent the fractional areas open to flow, u, v, and w represent the velocity components in x, y, and z directions or r, Θ, and z, c^2 represents the square of the sound, p represents the pressure, and R and ξ represent coordinates-dependent coefficients, for cartesian coordinates, they are set to unity and zero, respectively (Arun & Ritu, 2022; Hilo et al., 2021; Hilo et al., 2018; Flow science, 2014).

2.2. Meshing and Geometry

The 3-D models of the studied broad-crested weirs of various geometries were plotted by the assistance of the 3-D environment of AutoCAD 2016. The tested weirs were plotted typically like the previous experimental models of (Sargison & Percy, 2009). Using the lithography format (*.stl), the plotted AutoCAD models were exported to FLOW-3D program. Fig. 2 shows the three dimensional ARB broad-crested weir by AutoCAD.

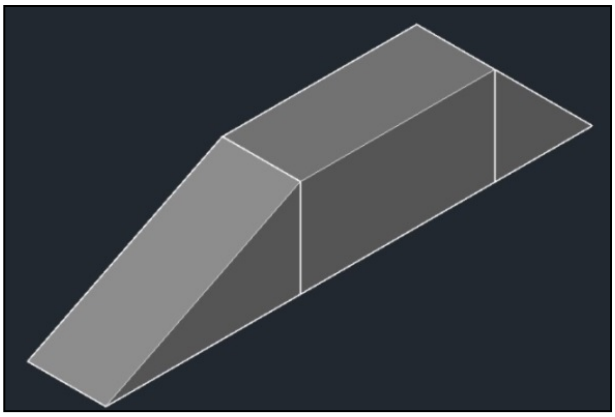

Figure 2. ARB weir by AutoCAD.

The numerical model consists of a horizontal flume. The cross section of the used flume was 200 mm wide and 5.4 m length, the tail water was remained at a small depth, which must not govern the oncoming water discharge for all the studied models. The investigated weir was built from three different sections: the rectangular crest, the downstream face, and the upstream face. The downstream and upstream parts can be altered to create various combinations of up- and downstream inclinations, while the crest length was fixed. The inclinations studied were 1H:1V, 2H:1V and V (vertical), all the used joint edges were. Fig. 3 presents the naming conventions, dimensions, and configurations for the studied model components.

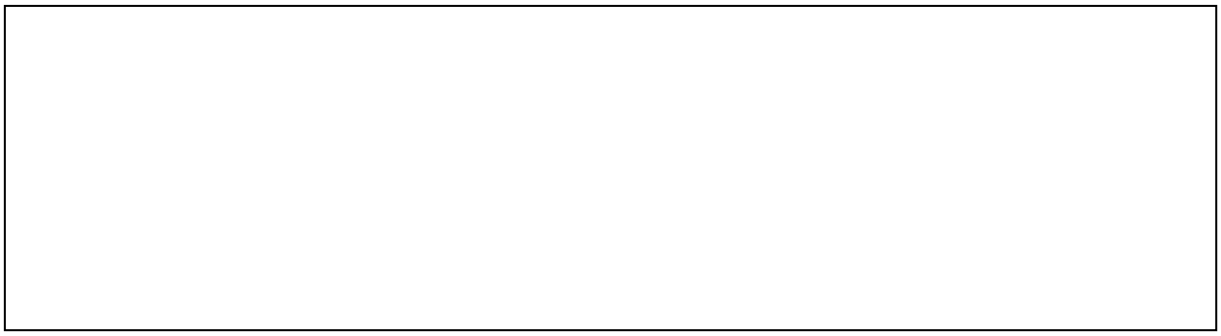

Figure 3. Dimensions, configurations, and naming convention for weir models (after Sargeson & Percy, 2009).

For achieving results with high accuracy, suitable number of cells should be selected. Actually, the accuracy of the obtained results significantly enhances as number of cells increases. However, the use of high number of cells considerably increases the time needed for the simulation process; therefore, a best number of cells should be chosen. FAVOR option is helpful for selecting the appropriate cell number and also for achieving adequate shape of model. The cells sizes for the studied weirs were 0.5, 0.83, 0.83 and 0.81 cm for ARB, BRA, VRB and BRV weirs, respectively. Fig. 4 shows the tested ARB weir model according to FAVOR.

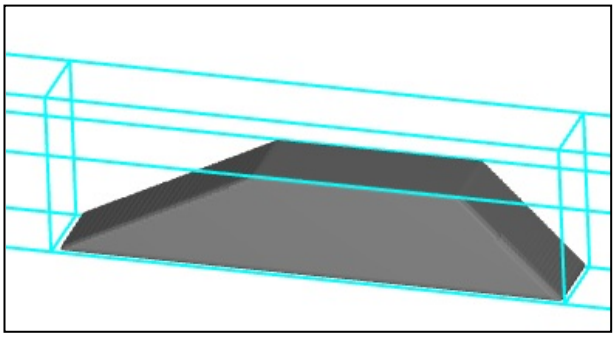

Figure 4. FLOW-3D model of the ARB weir by FAVOR.

2.3. Boundary and Initial Conditions

The solution of any model using FLOW-3D program is highly governed by finding the solution of the dominant fluid flow PDEs at the model's boundary and initial conditions; therefore, accurate results need precise simulations of the aforementioned conditions. In the current investigations, six boundary conditions, as depicted in Fig. 5, were used to provide adequate processes of simulation, they were:

X-max. (weir's downstream): Specified pressure (P).
X-min. (weir's upstream): Volumetric flow rate (Q).
Y-max. and Y-min. (weir's sides): Wall (W).
Z-max. (weir's top surface): Specified pressure (P).
Z-min. (weir's bottom surface): Wall (W).

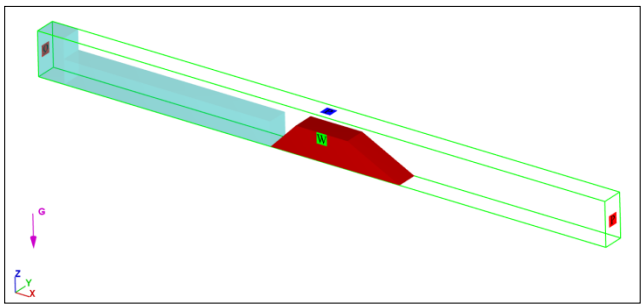

Figure 5. Boundary conditions of the BRA weir model.

2.4. Fluid Characteristics and Physics

In the present numerical study, the mass density of the used water was 1gm/cm^3, and its dynamic viscosity was 0.01gm/cm.sec, while its temperature was 20°C. For providing an accurate numerical simulation, three physics were activated. Density elevation was selected as a function of the remaining variables, the gravity was also selected, its value was -980 cm/sec^2 in z-axis, and finally the viscous flow was activated. CFD solution is highly governed by the choose of the appropriate model of turbulence. The last is controlled by various considerations such as the physics included in fluid flow, the required level of accuracy, the performed practice for a specific problem kind, the obtainable computation resources, and the preferable time of simulation. The k-ε model was depended in this study; it can be considered the most commonly used and validated model of turbulence (Abimbola, 2018).

3. Numerical Results

3.1. Verification Process

As aforementioned earlier, the current numerical study was based on the laboratory work of (Sargison & Percy, 2009). The numerical value of h_1, which represents upstream water depth above the crest, was used for verification purpose. To determine the difference

percentage between the numerical and experimental results, the following formula was used:

$$\text{Difference } \% = \frac{h_{1Exp.} - h_{1Num.}}{h_{1Exp.}} \times 100\% \quad (5)$$

where, $h_{1Exp.}$ and $h_{1Num.}$ represent the experimental and numerical value of h_1.

Fig. 6 shows the obtained results of verification process for the various weir geometry due to different applied discharges (Run). The results revealed that the determined differences were in the range between 0.0% for ARB weir when the applied discharge was 0.0055 m^3/sec to 9.6% for VRB weir when the applied discharge was 0.0056 m^3/sec. This can be considered acceptable result as they were less than 10% (Huan et al., 2011).

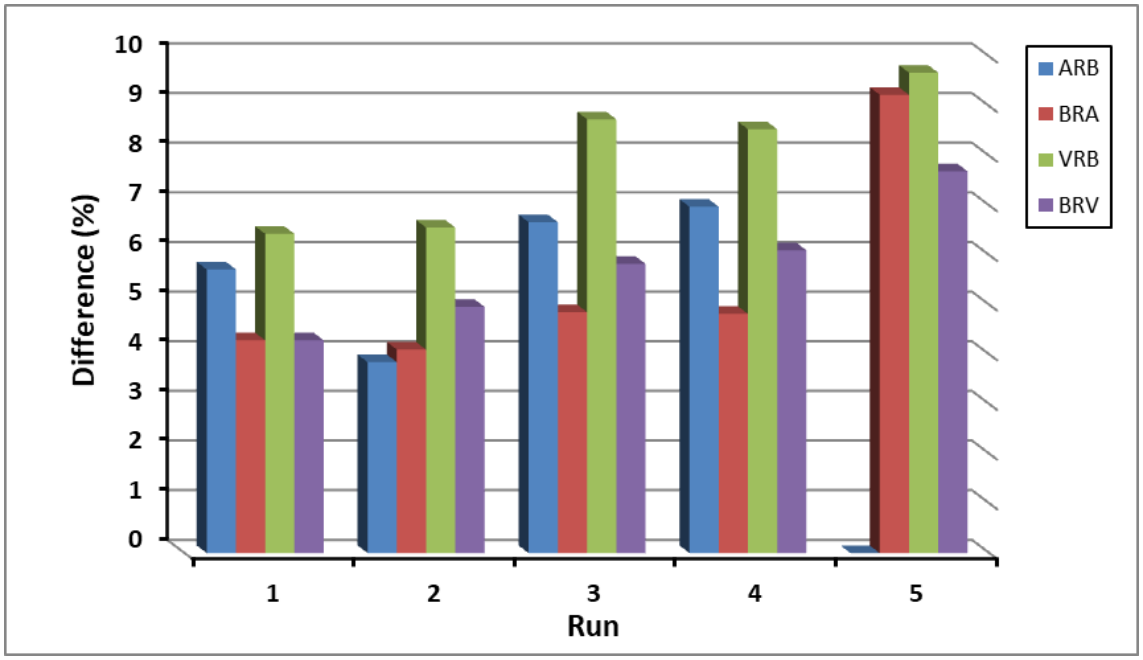

Figure 6. Verification process results.

Figs. 7 to 10 present the numerical and experimental h_1 values for ARB, BRA, VRB, and BRV weirs, respectively. It is obvious that the obtained numerical results were slightly lower than the experimental values for all the studied weir geometries; the average difference was 5.9%.

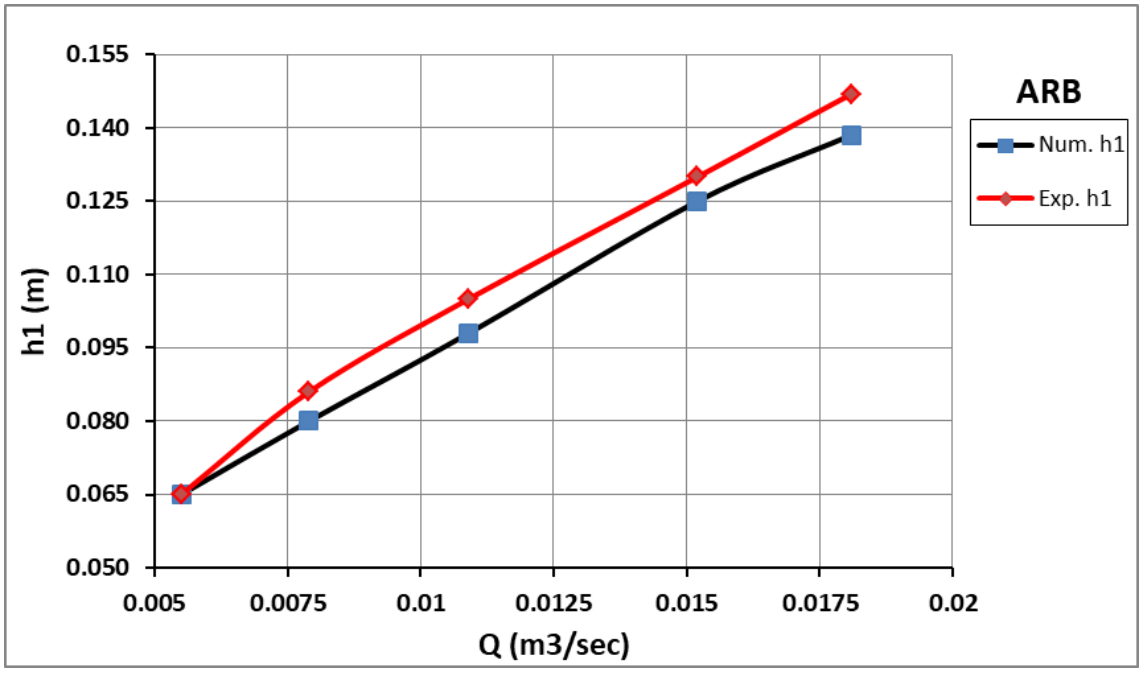

Figure 7. Experimental and numerical values of h_1 for ARB weir.

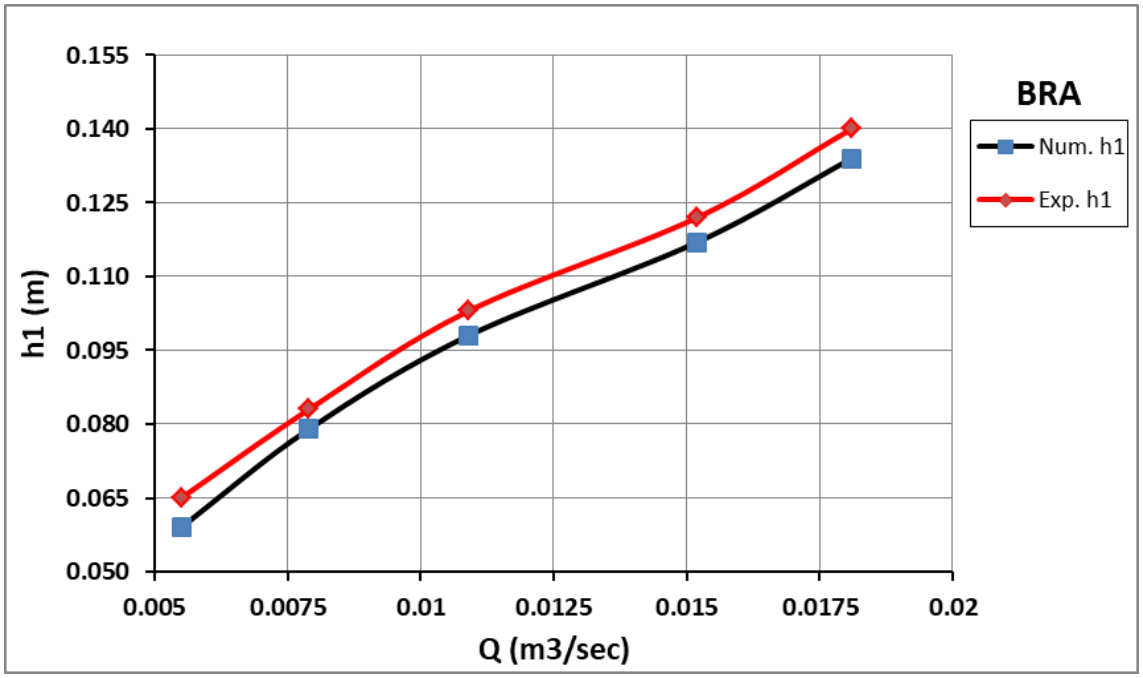

Figure 8. Experimental and numerical values of h_1 for BRA weir.

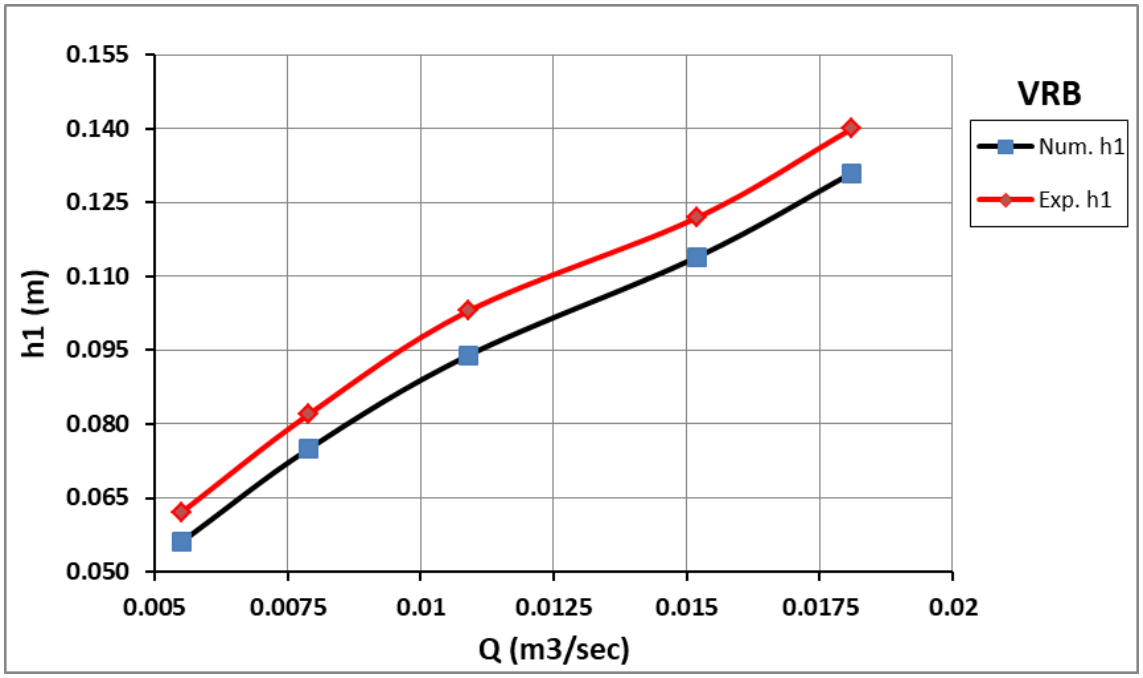

Figure 9. Experimental and numerical values of h_1 for VRB weir.

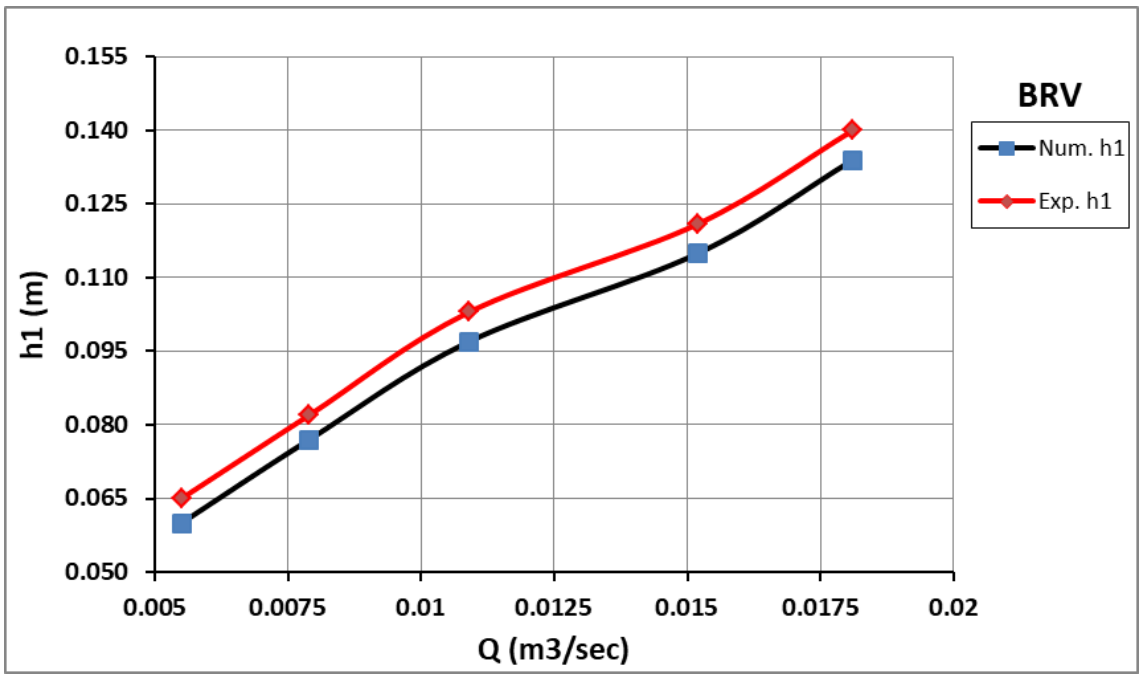

Figure 10. Experimental and numerical values of h_1 for BRV weir.

3.2. Discharge coefficient (C_d)

In the current study, the coefficient of discharge was determined using two well-known equations. Due to (Hager & Schwalt, 1994), discharge coefficient can be determined by the following equation:

$$Q = C_d \times b \times \sqrt{2gH_1^3} \quad (6)$$

where,

Q: flow discharge (L^3/T).

C_d: coefficient of discharge (dimensionless).

b: length of weir normal to the flow (L).

g: gravity acceleration (L/T^2).

H_1: upstream total energy above crest of the weir (energy grade line), which can be calculated by the following formula according to (Hager & Schwalt, 1994):

$$H_1 = h_1 + [Q^2/2gb^2(h_1 + P)^2] \quad (7)$$

where: P represents the weir height.

Additionally, coefficient of discharge was also calculated depending on Bazin's equation that takes into account the effect of upstream inclination (Bazin, 1898):

$$C_d = 0.43 + 0.06\sin[\pi(\varepsilon - 0.55)] - 0.0396\theta + 0.0029 \quad (8)$$

where,

ε: relative length of crest, it can be calculated by:

$$\varepsilon = H_1/(H_1 + w) \quad (9)$$

where,

w: the length of horizontal part of the weir parallel to the flow.

θ: upstream angle (rad).

The coefficients of discharge results for different weirs are shown in Figs. 11 to 14. One can conclude clearly that Hager's equation produced C_d values higher than that of Bazin's for all applied flow discharges and various shapes of weir. Furthermore, Hager's discharge coefficient exhibited an obvious fluctuation with discharge, there were no a distinct relationship between C_d value and discharge. On the other hand, the relationship between Bazin's equation and flow discharge for all studied cases were linear, C_d increases significantly as flow discharges increases.

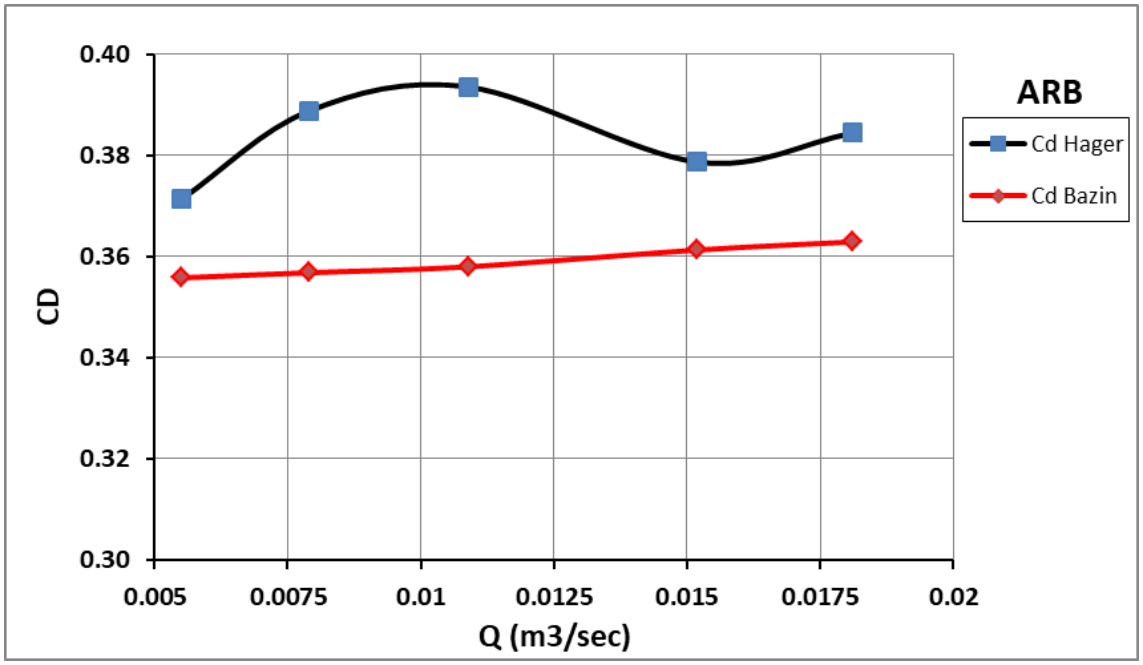

Figure 11. The calculated C_d values for ARB weir.

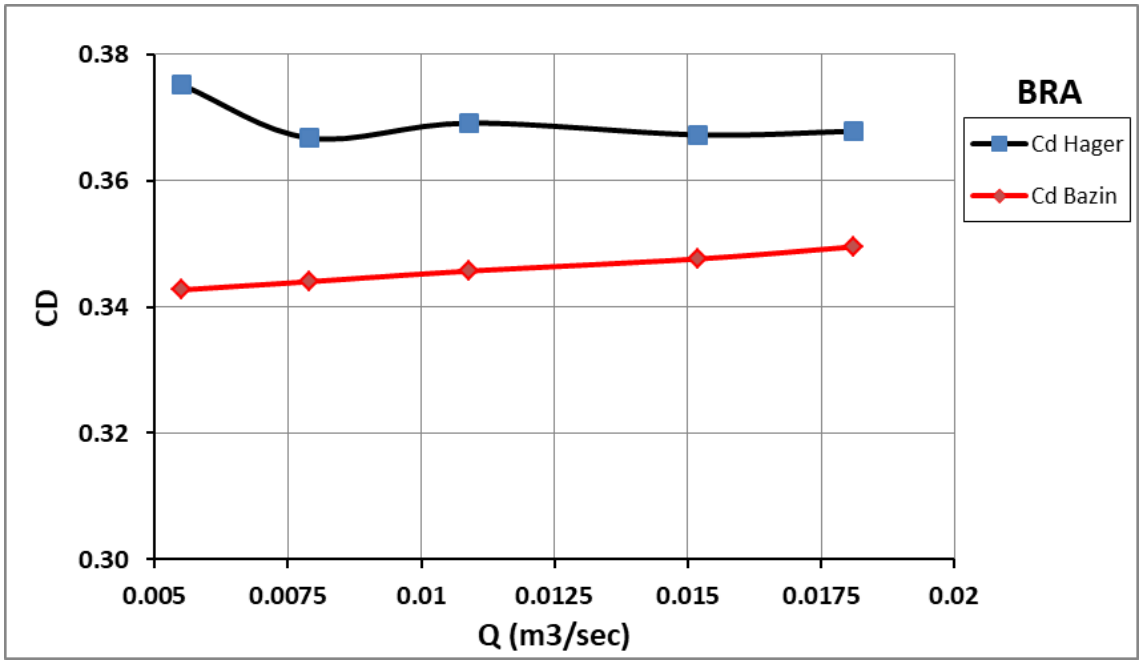

Figure 12. The calculated C_d values for BRA weir.

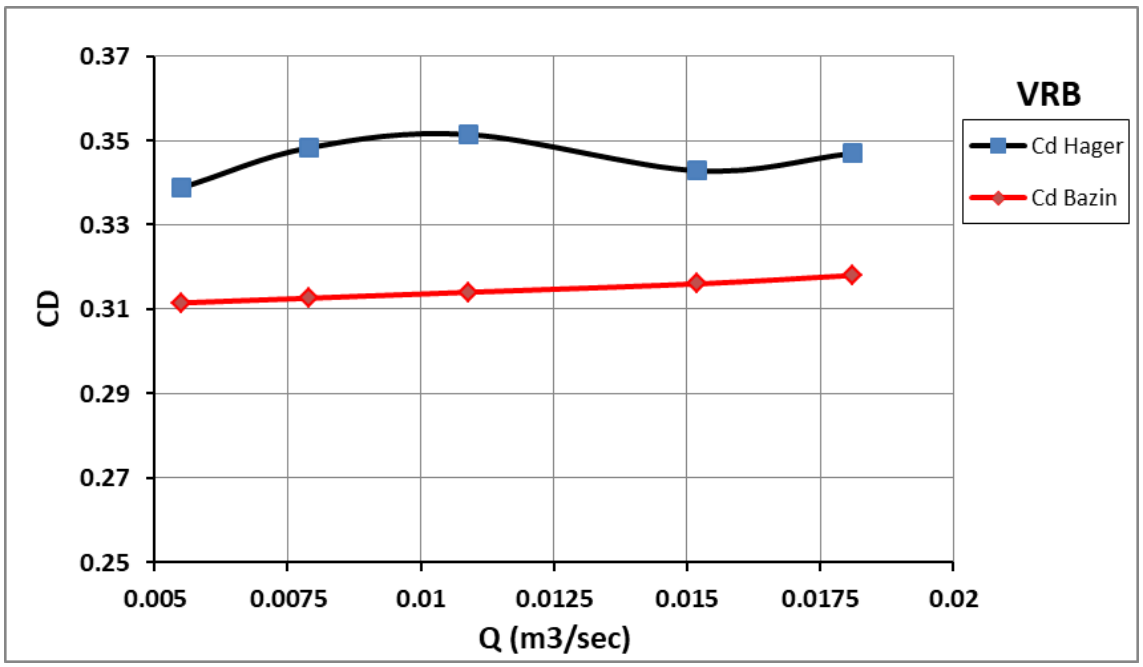

Figure 13. The calculated C_d values for VRB weir.

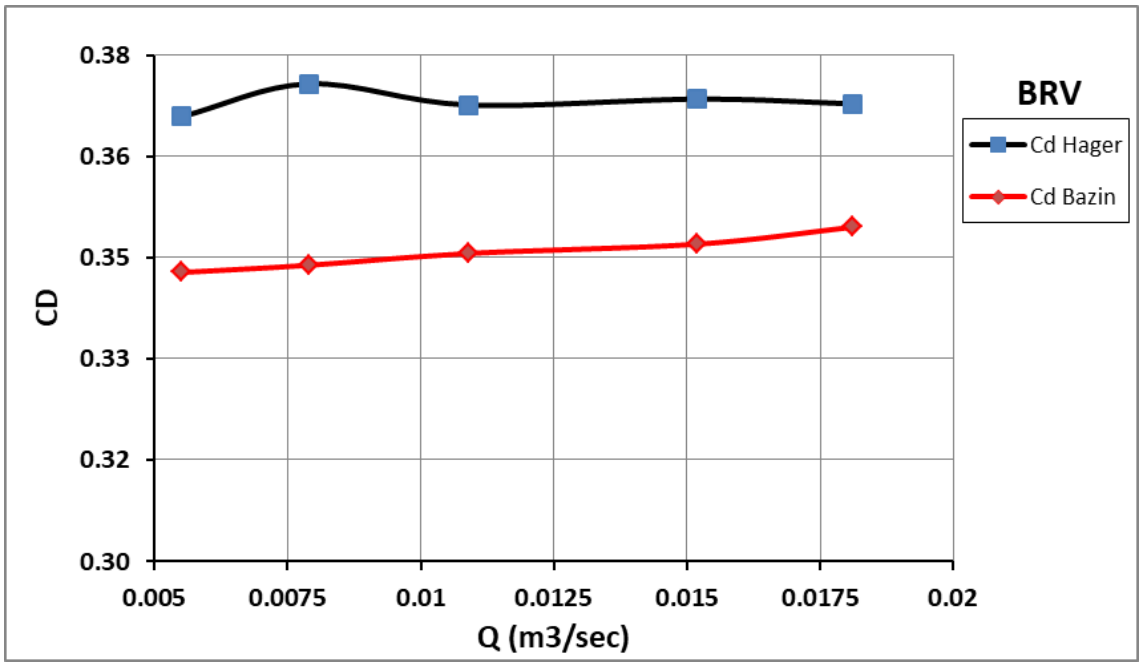

Figure 14. The calculated C_d values for BRV weir.

The effect of applied flow discharge on the resulted Bazin's discharge coefficient for various weir geometries is depicted in Fig. 15. It is obvious that the increment of discharge increases slightly the C_d value for all studied weir shapes. For ARB weir, C_d was 0.356, 0.357, 0.358, 0.361, and 0.363 when the discharges of 0.0055, 0.0079, 0.0109, 0.0152, and 0.0181 m^3/sec were applied, respectively. On the other hand, for VRB weir, it was 0.311, 0.313, 0.316, and 0.318 for discharges of 0.004, 0.0064, 0.0091, 0.0119, and 0.149 m^3/sec.

Furthermore, the weir ARB showed the highest discharge coefficient value, the average value was 0.359, while VRB weir exhibited the lowest with an average of 0.314. This indicates definitely that for the same downstream condition, reducing upstream inclination increases C_d value. For weirs of BRA and BRV, the average discharge coefficient was quit close, this revealed undoubtedly that for the same upstream inclination, downstream slope had a negligible effect of the value of C_d. For a constant discharge value, as the slope of upstream face reduced by 50 and 70.5%, the coefficient of discharge increased approximately by 9.5 and 13.2%, respectively.

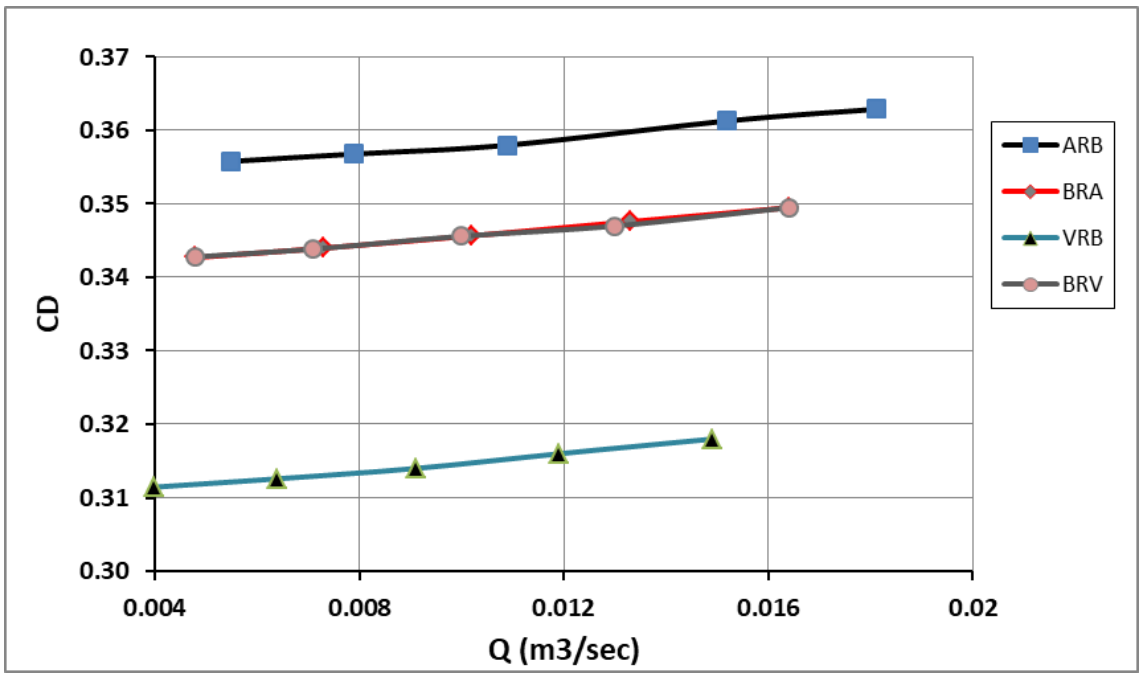

Figure 15. The calculated C_d values for various weirs.

Finally, the relationship between discharge coefficient and relative crest length for various weirs was shown in Fig. 16.

For the same value of relative crest length (ε), value of discharge coefficient was higher for the lower upstream slope, and it was approximately the same for the typical upstream inclination regardless the downstream shape. Tab. 1 presents the results of discharge coefficients.

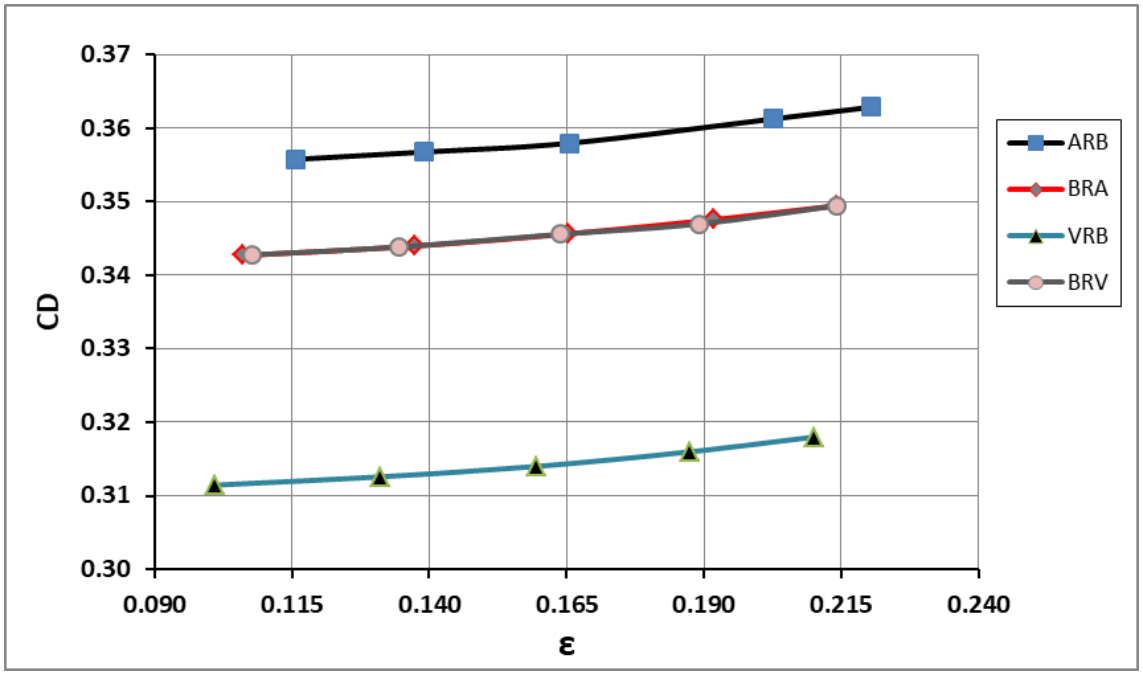

Figure 16. The relationship between C_d values and ε for various weirs.

Table1. Results of discharge coefficients.

Weir	Q (m^3/sec)	C_d Hager	ε	C_d Bazin
ARB	0.0181	0.384	0.220	0.363
	0.0152	0.379	0.203	0.361
	0.0109	0.394	0.166	0.358
	0.0079	0.389	0.139	0.357
	0.0055	0.371	0.116	0.356
BRA	0.0164	0.368	0.214	0.350
	0.0133	0.367	0.192	0.348
	0.0102	0.369	0.165	0.346
	0.0073	0.367	0.137	0.344
	0.0048	0.375	0.106	0.343
VRB	0.0149	0.347	0.210	0.318
	0.0119	0.343	0.187	0.316
	0.0091	0.351	0.160	0.314
	0.0064	0.348	0.131	0.313
	0.004	0.339	0.101	0.311
BRV	0.0164	0.368	0.214	0.350
	0.013	0.368	0.189	0.347
	0.01	0.368	0.164	0.346
	0.0071	0.371	0.134	0.344
	0.0048	0.366	0.108	0.343

3.3. Energy Grade Line (H_1)

The upstream energy grade line was calculated using Eq. 7. The resulted upstream energy grade line (H_1) against the applied flow discharges for the studied weirs is shown in Fig. 17. The obtained value of H_1 was governed totally by the upstream slope, it increased due to the increment of the inclination, while the influence of downstream inclination was approximately negligible. For the same applied flow discharge, value of H_1 was the highest for VRB weir, while it exhibited the lowest value for ARB weir. Weirs of BRV and VRB showed the same upstream energy grade line value. It can be concluded also that as the flow discharge increased, the effect of upstream shape increased. Tab. 2 lists the obtained H_1 results.

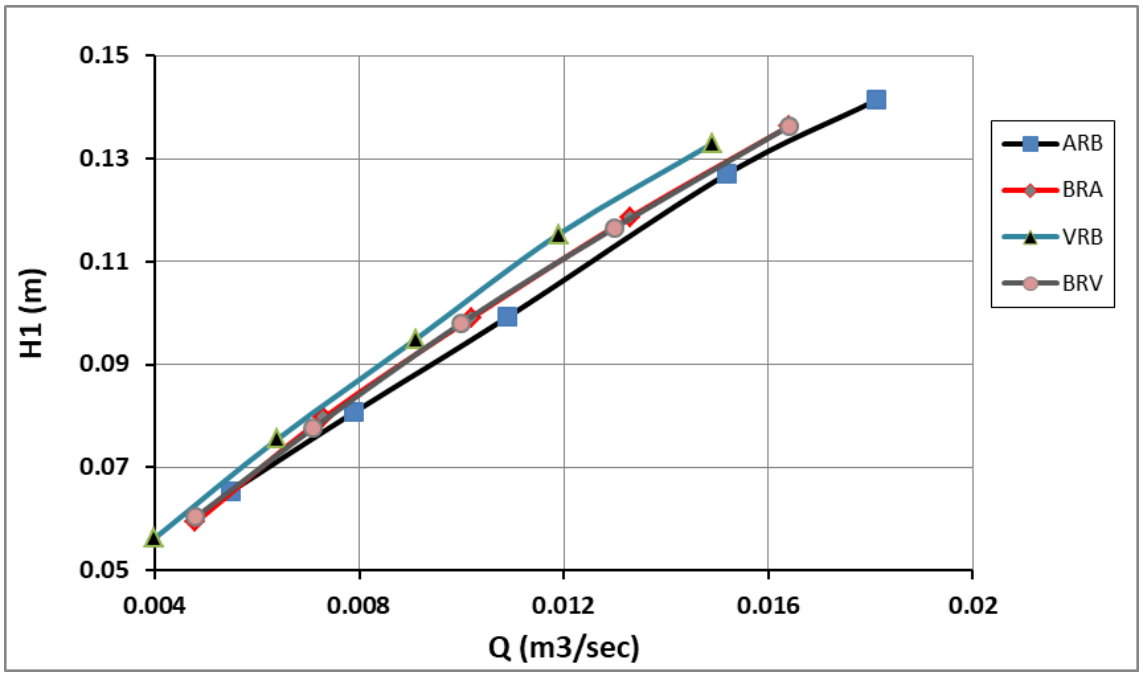

Figure 17. The relationship between H_1 values and Q for various weirs.

Table 2. Results of upstream energy grade line.

Weir	Q (m^3/sec)	Num. h_1 (m)	H_1 (m)
ARB	0.0181	0.139	0.141
	0.0152	0.125	0.127
	0.0109	0.098	0.099
	0.0079	0.080	0.081
	0.0055	0.065	0.0654
BRA	0.0164	0.134	0.136
	0.0133	0.117	0.119
	0.0102	0.098	0.099
	0.0073	0.079	0.080
	0.0048	0.059	0.059
VRB	0.0149	0.131	0.133
	0.0119	0.114	0.115
	0.0091	0.094	0.095
	0.0064	0.075	0.075
	0.004	0.056	0.056
BRV	0.0164	0.134	0.136
	0.013	0.115	0.117
	0.01	0.097	0.098
	0.0071	0.077	0.078
	0.0048	0.060	0.060

3.4. Flow Velocity

The depth-averaged velocity curves along the used flume can be obtained using FLOW-3D program. Fig. 18 shows these curves when the flow discharges were 0.0055, 0.0048, 0.0048, and 0.004 m^3/sec for ARB, BRA, BRV, and VRB weir, respectively. It is worth mentioning that zero point on the abscissa represents the beginning of the weir. Although the discharge for ARB weir was higher than that of VRB by 27.3%, its maximum flow velocity was lower by 1.6%. Thus, it can be concluded that increasing upstream inclination for the same downstream slope increases the resulted flow velocity. Furthermore, for the same applied discharge (0.0048 m^3/sec), BRV weir exhibited flow velocity lower than that of BRA by 28%. One can notice that for the same upstream inclination and flow discharge, increasing downstream slope reduces the flow velocity. As a result, abrasion erosion and scour depth can be reduced considerable as flow velocity reduced (Abid et al., 2019; ACI Committee 210, 2003).

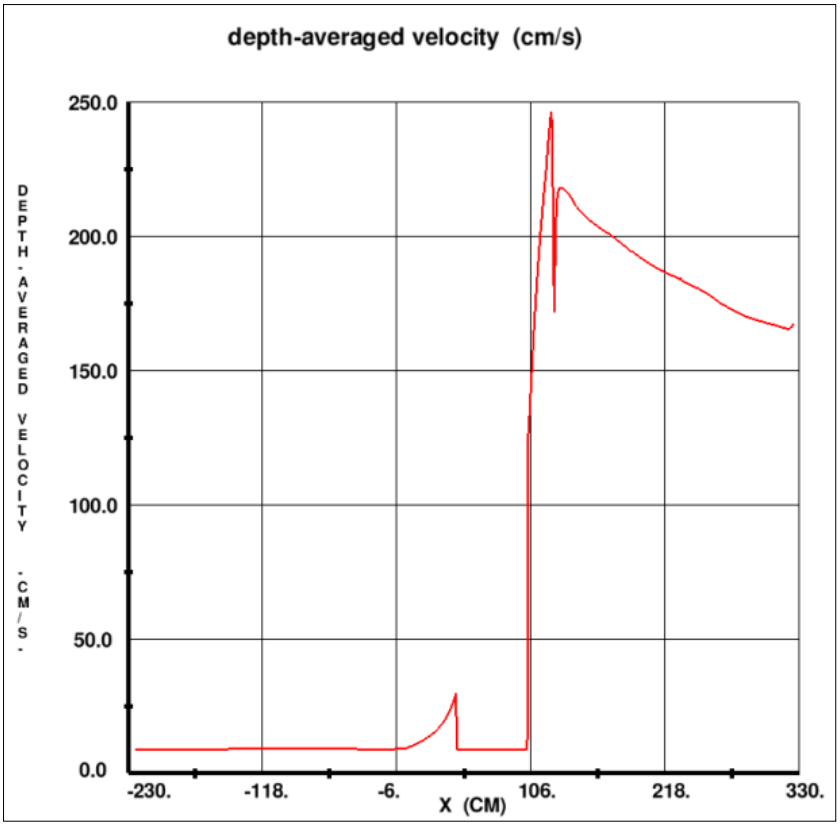
depth-averaged velocity (cm/s)
DEPTH-AVERAGED VELOCITY -CM/S-
250.0
200.0
150.0
100.0
50.0
0.0
-230.
-118.
-6.
106.
218.
330.
X (CM)

(a)

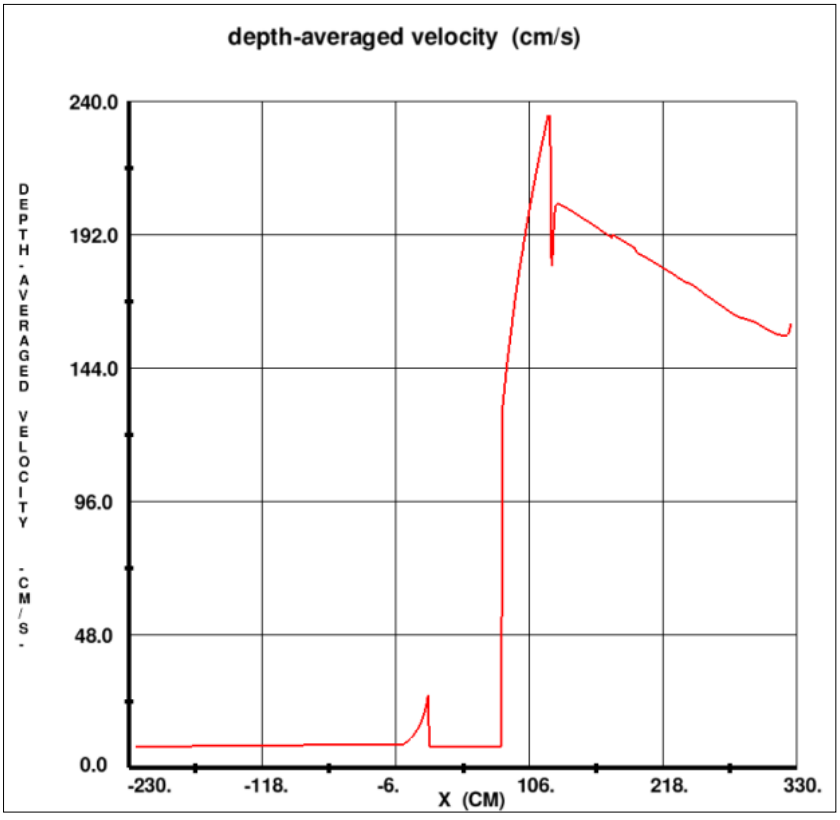
depth-averaged velocity (cm/s)
DEPTH-AVERAGED VELOCITY -CM/S-
240.0
192.0
144.0
96.0
48.0
0.0
-230.
-118.
-6.
106.
218.
330.
X (CM)

(b)

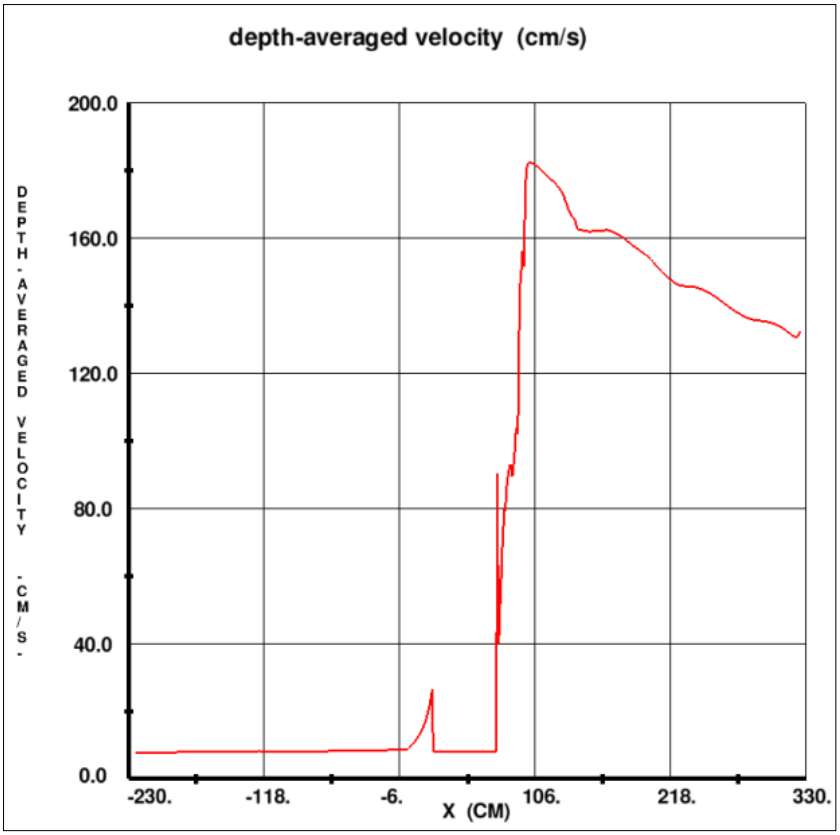

(c)

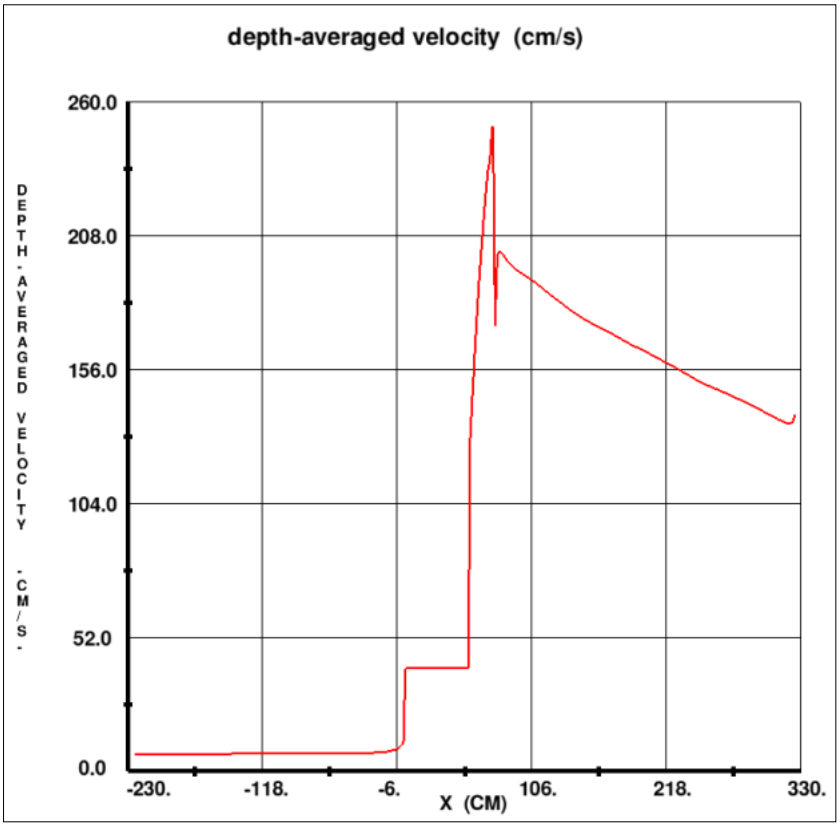

(d)

Figure 18. Depth-averaged velocity for (a) ARB (b) BRA (c) BRV and (d) VRB weir.

4. Conclusions

The current numerical study was carried out using FLOW-3D v11.0.4 software to check the suitability and applicability of CFD programs to simulate the complex water flow over broad-crested weirs of different shapes. Four weir geometries were studied, the horizontal crest was constant but the upstream and downstream faces were variant. According to the results of this investigation, the following points represent the main conclusions:

1) FLOW-3D is able adequately to simulate the free flow features over broad-crested weir. The obtained difference percentages between the experimental and numerical h_1 results were between 0.0 and 9.6% with an average of 5.97%.
2) According to coefficient of discharge determinations:
   A. For the same weir geometry, Bazin's discharge coefficient increases slightly by the increment of flow discharge. For ARB weir, the C_d value increased approximately 2% when the flow discharge increased by 69.6%. Hager's discharge coefficient shows unstable relationship with discharge.
   B. When conditions of downstream face are the same, increasing the upstream slope reduces the coefficient of discharge considerably.
   C. Downstream condition has a negligible influence on the discharge coefficient.
   D. As the relative crest length increases, the coefficient of discharge enhances.
3) The energy grade line increases as the slope of upstream increases, while downstream face shows no effect.
4) For the same downstream slope, as upstream slope decreases, the flow velocity also decreases. Moreover, for the same upstream slope, the increment of downstream inclination reduces the resulted velocity.

REFERENCES

[1] Abid, S. R., Hilo, A. N., Ayoob, N.S. and Daek Y. H. (2019). "Underwater abrasion of steel fiber-reinforced self-compacting concrete", *Case Studies in Construction Materials*, vol. 11, pp. 1-17.

[2] Abimbola, A. O. (2018). "Wave propagation and scour failure of coastal structures due to tsunamis", *Ph.D thesis*.

[3] ACI Committee 210. (2003). "Erosion of concrete in hydraulic structure (ACI 210R-03)", *American concrete institute, USA*, pp. 1-24.

[4] Arun, K. and Ritu, R. (2022). "CFD Study of Flow Characteristics and Pressure Distribution on Re-Entrant Wing Faces of L-Shape Buildings". *Civil Engineering and Architecture*, vol. 10(1), pp. 289-304. DOI: 10.13189/cea.2022.100125

[5] Azimi, A. H. and Rajaratnam, N. (2009). "Discharge characteristics of weirs of finite crest length", *Journal of Hydraulic Engineering*, vol. 135(12), pp. 1081-1085.

[6] Bazin, H. (1898). "Experience nouvelles sur l' ecoulement en deversoir", *Ann. Ponts chausses*, vol. 68(2), pp. 151-265.

[7] BSI (1969b). *Measurement of Liquid Flow in Open Channels: Weirs and Flumes*, BS 3680, Part 4, British Standards Institution, London.

[8] Chow, V.T., 1959. *Open-channel hydraulics*, McGraw-Hill.

[9] Flow Science. (2014). "FLOW-3D version 11 user manual".

[10] Fritz, H. M. and Hager, W. H. (1998). "Hydraulics of embankment weirs", *Journal of Hydraulic Engineering*, vol. 124(9), pp. 963-971.

[11] Gonzalez, C. A. and Chanson, H. (2007). "Experimental measurements of velocity and pressure distribution on large broad-crested weir", *Flow measurement and Instrumentation*, vol., pp. 107-113.

[12] Hager, W. H. and Schwalt, M. (1994). "Broad-crested weir", *Journal of Irrigation and Drainage Engineering*, vol. 120(1), pp. 13-26.

[13] Haun, S., Olsen, N. R. B. and Feurich, R. (2011). "Numerical modeling of flow over trapezoidal broad-crested weir", *Engineering Applications of Computational Fluid Mechanics*, vol. 5(3), pp. 397-405.

[14] Hilo, A. N., Ayoob, N. S. and Daek, Y. H. (2021). Numerical Simulation to Evaluate The Effect of The Stepped Chute on Abrasion Erosion of A Stilling Basin Type III. *IOP Conference Series: Materials Science and Engineering,* vol. 1090, pp. 1-11.

[15] Hilo, A. N., Abid, S. R. and Daek, Y. H. (2018). Numerical Model for Flow on Stilling Basin Type III. *International Conference on Advances in Sustainable Engineering and Applications (ICASEA)*, pp. 126-130.

[16] Ramamurthy, A. S., Tim, U. S. and Rao, M. V. J. (1988). "Characteristics of square-edged and round-nosed broad-crested weir", *Journal of Irrigation and Drainage Engineering*, vol. 114(1), pp. 61-72.

[17] Sargison, J. E. and Percy, A. (2009). "Hydraulics of broad-crested weirs with varying side slopes", *Journal of Irrigation and Drainage Engineering*, vol. 135(1), pp. 115-118.

[18] Sarker, M. A. and Rhodes, D. G. (2004). "Calculation of free-surface profile over a rectangular broad-crested weir", *Flow Measurement and Instrumentation*, vol. 15, pp. 215-219.